A Computational Framework for Experimental Design in Diffusion MRI

Emmanuel Caruyer, Rachid Deriche

▶ To cite this version:

HAL Id: hal-00747700

https://inria.hal.science/hal-00747700

Submitted on 1 Nov 2012

A Computational Framework for Experimental Design in Diffusion MRI

Emmanuel Caruyer, Rachid Deriche

Athena Project-Team, Inria Sophia Antipolis - Méditerranée
2004 Route des Lucioles - 06902 Sophia Antipolis Cedex - France

Abstract. In this work, we develop a computational framework for optimal design of experiment in parametric signal reconstruction. We apply this to the optimal design of one dimensional q-space, q-ball imaging and multiple q-shell experimental design. We present how to construct sampling scheme leading to minimal condition number, and compare to state-of-the-art sampling methods. We show in particular a better noise performance of these scheme through Monte-Carlo simulations for the reconstruction of synthetic signal. This demonstrates the impact of this computational framework on acquisition in diffusion MRI.

1 Introduction

Diffusion MRI investigates the properties of tissue microstructure from the analysis of water molecules displacement. The diffusion characteristics, such as the ensemble average propagator or the orientation distribution function, are related to the diffusion signal attenuation through continuous transforms. Since then, the first step in the processing pipeline is usually a parametric estimation of the diffusion signal, from a series of discrete measurements. The number of samples in diffusion MRI is limited to keep the acquisition time compatible with in-vivo measurements. Therefore, the choice of sampling points in the q-space is critical for a proper reconstruction and quantitative analysis of diffusion characteristics.

The question of sampling efficiency has been widely studied for parametric estimation in diffusion MRI. Several approaches were proposed to uniformly arrange points on the sphere in q-ball imaging (QBI), using an analogy between the sampling directions and a pair of antipodal electric charges [1, 2], or geometric constructions [3]. For the reconstruction of diffusion tensor MRI, the noise performance has been studied through the minimization of the condition number [4, 5]. In q-space MRI, several studies on multiple shell sampling [6–9] focused on the efficiency of various sampling strategies, but they do not provide a method to systematically improve the noise performance.

In this work, we give a general method for optimal design of experiment in parametric signal reconstruction. We apply this to the optimal design on one dimensional q-space experiment, q-ball imaging and multiple q-shell experimental design. In the last section, we compare the proposed method to state-of-the-art sampling strategies.

2 Theory

2.1 Parametric estimation of the diffusion signal

The diffusion signal is approximated in a finite, orthonormal basis of functions

$$\forall \mathbf{q} \in \Omega, \qquad E(\mathbf{q}) = \sum_{i=1}^{R} c_i f_i(\mathbf{q}), \tag{1}$$

where $\Omega \subset \mathbb{R}^3$. Depending on the application, we have $\Omega = \mathbb{R}$ (1D diffusion signal), $\Omega = \mathcal{S}^2$ (QBI) or $\Omega = \mathbb{R}^3$ (q-space imaging).

Provided K measurements $y_k = E(\mathbf{q}_k)$ of the signal at wavevectors $\mathbf{q}_k$, the coefficients $\hat{c}_i$ are estimated by least squares. Put in matrix form, we write

$$\hat{\mathbf{c}} = (\mathbf{H}^{\mathrm{T}}\mathbf{H})^{-1}\mathbf{H}^{\mathrm{T}}\mathbf{y}. \tag{2}$$

$\mathbf{H}$ is the design matrix, and has entries $H_{ki} = f_i(\mathbf{q}_k)$.

2.2 Information matrix and optimal design

We present a general method to choose the sampling points $\mathbf{q}_k$ to optimize the noise performance. A useful index for noise performance and stability of the reconstruction is the condition number $\kappa(\mathbf{M}) = \lambda_{\max}(\mathbf{M})/\lambda_{\min}(\mathbf{M})$ of the information matrix $\mathbf{M} = 1/K\ \mathbf{H}^{\mathrm{T}}\mathbf{H}$, where K is the number of measurements. The condition number is an upper bound to the error propagation from the measurements to the coefficients estimates. The optimal value of $\kappa(\mathbf{M})$ is 1, in which case the information matrix is proportional to the identity $\mathbf{I}_R$.

The coefficients of the information matrix M_{ij} can be interpreted as the approximation of the continuous dot product $\langle f_i, f_j \rangle$

$$M_{ij} = \frac{1}{K} \sum_{k=1}^{K} f_i(\mathbf{q}_k) f_j(\mathbf{q}_k) \approx \int_{\Omega} f_i(\mathbf{q}) f_j(\mathbf{q}) \mathrm{d}\Omega(\mathbf{q}) = \delta_{ij} \tag{3}$$

The basis is orthonormal, hence if this approximation is exact, $\mathbf{M} = \mathbf{I}_R$, and the associated condition number equals 1. This naturally introduces the notion of quadrature formula, and its generalization to higher dimension, called the cubature formula.

Definition 1. *A cubature formula for the integral $\mathcal{I} = \int_{\Omega} g(\mathbf{q})\mathrm{d}\Omega(\mathbf{q})$ is a collection of nodes $\mathbf{q}_s$ and weights ω_s such that*

$$\mathcal{I} = \sum_{s=1}^{S} \omega_s g(\mathbf{q}_s) \tag{4}$$

If such a cubature formula exists for the integral in Eq. 3, then we place the sampling points at nodes $\mathbf{q}_s$, and the number of repetitions K_s at node $\mathbf{q}_s$ is proportional to the weight ω_s.

3 Methods

In this section, we derive cubature formulae for the simple harmonic oscillator basis [10] (1D diffusion signal), spherical harmonic basis [11] (QBI) and spherical polar Fourier basis [12] (q-space imaging).

### 3.1 Optimal design in one dimensional q-space MRI

The simple harmonic oscillator basis for the reconstruction of real diffusion signal in one dimension [10] is given by $\Phi_i(q, u) = \kappa_i(u) \exp(-2\pi^2 q^2 u^2) L_i^{-1/2}(4\pi^2 q^2 u^2)$, where u is a characteristic length, $L_i^{-1/2}$ the generalized Laguerre polynomial of degree i and $\kappa_i(u)$ a normalization constant.

Put back into the general framework presented in Section 2.2, we have $\Omega = \mathbb{R}$, and the basis functions are $f_i = \Phi_i$. For the evaluation of the dot product in Eq. 3, we use the substitution $x = 4\pi^2 q^2 u^2$, so that

$$\langle \Phi_i, \Phi_j \rangle = 2\pi u \kappa_i(u) \kappa_j(u) \int_0^\infty L_i^{-1/2}(x) L_j^{-1/2}(x) x^{-1/2} e^{-x} \mathrm{d}x. \tag{5}$$

When the basis is truncated to order N, the evaluation of Eq. 5 reduces to the problem of Gauss-Laguerre quadrature [13]. The optimal samples are $q_s = \sqrt{x_s}/2\pi u$, with K_s repetitions, where K_s is proportional to $x_s e^{x_s}/[L_N^{-1/2}(x_s)]^2$ and the nodes $x_s, s = 1 \ldots N + 1$ are the roots of $L_{N+1}^{-1/2}$.

3.2 Optimal design in q-ball imaging

| Geometric | Electrostatic | Optimal ($L = 4$) |
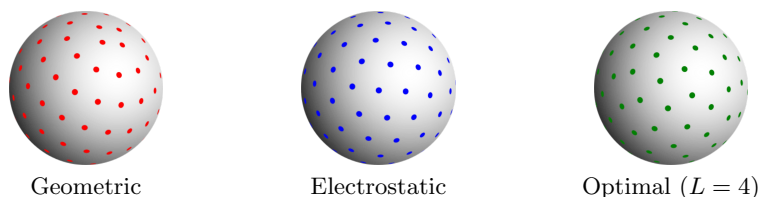
Fig. 1. Arrangements of $K = 50$ points on the unit sphere.

The real, symmetric spherical harmonic basis $\{Y_{lm}\}$ truncated to order L has dimension $R = (L+1) \cdot (L+2)/2$. Put back into the general framework presented in Section 2.2, we have $\Omega = \mathcal{S}^2$, and the basis functions are $f_i = Y_i$, where $i(l, m) = 1, 2, \ldots, R$ for $(l, m) = (0, 0), (2, -2), \ldots, (L, L)$.

This basis is equivalent to the basis of harmonic polynomial of degree L on $\mathcal{S}^2$, for which cubature formulae exist and are called spherical design.
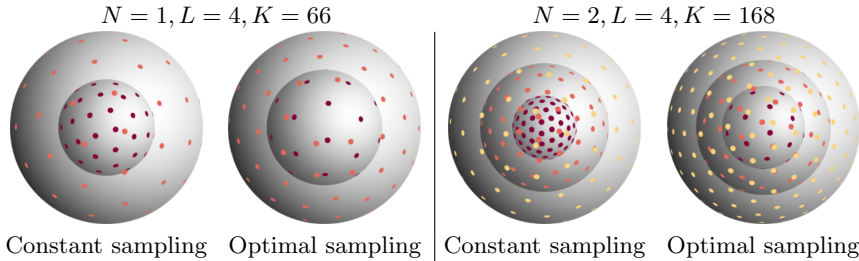
Definition 2. *A spherical t-design [14] is a sequence of K points $\mathcal{X} = (\mathbf{u}_k)$, $k = 1 \ldots K$ on the unit sphere, such that the integral of any polynomial $p(x, y, z)$*

of degree at most t over the sphere is equal to the average value of the polynomial on $\mathcal{X}$:

$$\frac{1}{K} \sum_{k=1}^{K} p(u_{kx}, u_{ky}, u_{kz}) = \int_{\mathcal{S}^2} p(\omega) \mathrm{d}^2 \omega. \tag{6}$$

If the sampling directions $\mathbf{u}_k$ form a spherical $2L$-design, then the approximation in Eq. 3 is exact and $\kappa(\mathbf{M}) = 1$. For the construction of a spherical $2L$-design with antipodal symmetry, we rely here on the equivalence criterion in [15]. An example of optimal direction set for order $L = 4$ is presented on Fig. 1, and compared to a geometric [3] and an electrostatic [1, 2] arrangements of points.

3.3 Optimal design in q-space imaging

$$N = 1, L = 4, K = 66 \qquad\qquad N = 2, L = 4, K = 168$$

Constant sampling Optimal sampling │ Constant sampling Optimal sampling

Fig. 2. 2-shell (left) and 3-shell (right) acquisition protocols: regular multiple q-shell with constant number of points per shell, and optimal arrangement with minimal condition number for reconstruction in SPF basis.

The truncated spherical polar Fourier (SPF) basis [12] is able to represent the diffusion signal in the whole q-space. To represent a continuous signal, which verifies $E(\mathbf{0}) = 1$, we have recently proposed a slightly modified version of the SPF basis [16]. We reconstruct the signal as $E(q \cdot \mathbf{u}) = \exp(-q^2/2\zeta) + \sum_{nlm} a_{nlm} C_{nlm}(q \cdot \mathbf{u})$. The basis functions are $C_{nlm}(q \cdot \mathbf{u}) = F_n(q) Y_{lm}(\mathbf{u})$, with

$$F_n(q) = \chi_n \frac{q^2}{\zeta} \exp\left(-\frac{q^2}{2\zeta}\right) L_n^{5/2}\left(\frac{q^2}{\zeta}\right), \tag{7}$$

ζ is a scale factor, χ_n a normalization constant, and Y_{lm} is the real spherical harmonic function. When the radial and angular truncation orders are N and L, respectively, this basis has dimension $R = N \cdot (L + 1) \cdot (L + 2)/2$. Put back into the general framework presented in Section 2.2, we have $\Omega = \mathbb{R}^3$, and the basis functions are $f_i = C_i$, where $i(n, l, m) = 1, 2, \ldots, R$ for $(n, l, m) = (0, 0, 0), (0, 2, -2), \ldots, (N, L, L)$.

For the construction of an optimal design for this basis, we build on the findings of the previous two sections. We show that the radial part of the integral in Eq. 3 reduces to a Gauss-Laguerre quadrature problem, while the angular part reduces to a spherical design problem.

Therefore we propose a design on $N + 1$ spheres in the q-space. The shell s has radius $q_s = \sqrt{\zeta x_s}$, where x_s is the sth root of $L_{N+1}^{5/2}$. The number of points K_s on shell s should be proportional to $\omega_s = \exp(-x_s)/[x_s(L_N^{5/2}(x_s))^2]$ Finally, the points on each sphere should form a spherical $2L$-design. Example of points sets generated with this method are depicted on Fig. 2. They are compared to multiple shell sampling where the shell radii are evenly spaced, and the number of points equal on each shell, as suggested in [7].

4 Experiments and Results

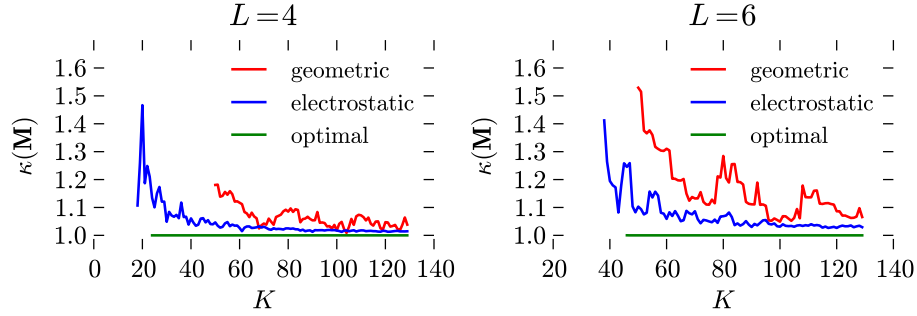### 4.1 Quadrature formula in one dimensional q-space MRI
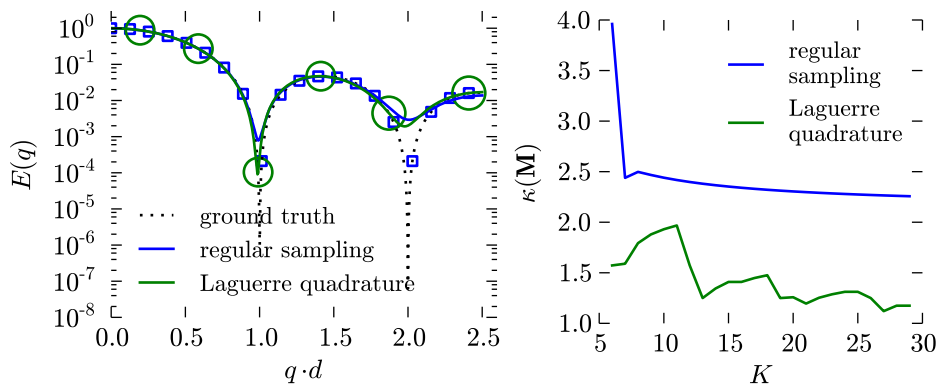
Fig. 3. Evaluation of Gauss-Laguerre quadrature for one dimensional q-space. (Left) An example of signal and its reconstruction. The blue squares and the green circles represent the regular and quadrature samples respectively. The radii of the circles are proportional to the number of repeated acquisitions. (Right) Condition number of the information matrix.

In this section, we show the feasibility of one dimensional q-space signal reconstruction from a set of measurements on a limited support size. We compare the Gauss-Laguerre quadrature to a regular sampling on the range $[0, q_{\max}]$

We plot on Fig. 3 an example of reconstruction of a diffusion signal corresponding to the restricted diffusion between two parallel planes, separated by distance d [10]. The truncation order in the basis was set to $N = 5$, and the corresponding Gauss-Laguerre quadrature works on 6 nodes. The result for a total of 20 acquisitions is visually identical to the reconstruction from a regular sampling. Besides, the associated information matrix is better conditioned for the quadrature sampling. The reason why the condition number is not exactly 1 in this case is that the quadrature weight ω_s is approximated by the number of repetitions at node q_s, which is an integer.

4.2 Evaluation of conventional schemes in q-ball imaging

We evaluate and report on Fig. 4 the noise performance of point sets generated with electrostatic analogy [1, 2] and by geometrical construction [3], for the reconstruction of SH coefficients of the diffusion signal. We compare these sampling methods to the proposed, optimal point set based on spheical design.

Fig. 4. q-ball imaging: condition number of the information matrix corresponding to the truncated SH up to order $L = 4$ (left) and $L = 6$ (right), of the electrostatic, geometric and optimal point sets. The geometric configurations are only provided for $K \geq 50$, as this method is reported to be dedicated to large K by the author in [3]. Our proposed, optimal design is based on spherical design, and therefore exists for $K \geq 24$ at order $L = 4$, and for $K \geq 46$ at order $L = 6$ [15]. By construction, the condition number associated is exactly 1.

## 4.3 Multiple q-shell and three dimensional signal reconstruction
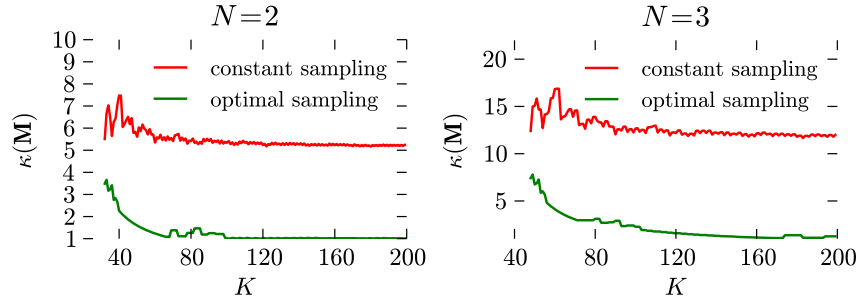
Fig. 5. Condition number of multiple shell sampling, corresponding to the SPF basis.

Using the results on Gauss-Laguerre quadrature and spherical designs, we generated optimal sampling schemes on multiple shells for the reconstruction in

the SPF basis. We compare this to the sampling strategy with shell radii evenly spaced and constant number of points per shell proposed in [7]. The condition number for the reconstruction in SPF basis is reported on Fig. 5.

We also simulate both methods, for the sampling and reconstruction of a synthetic diffusion signal corresponding to a mixture of Gaussian. Visual reconstruction is reported on Fig. 6, and quantitative comparison on Fig. 7.

| Ground truth signal | Constant sampling | Optimal sampling |
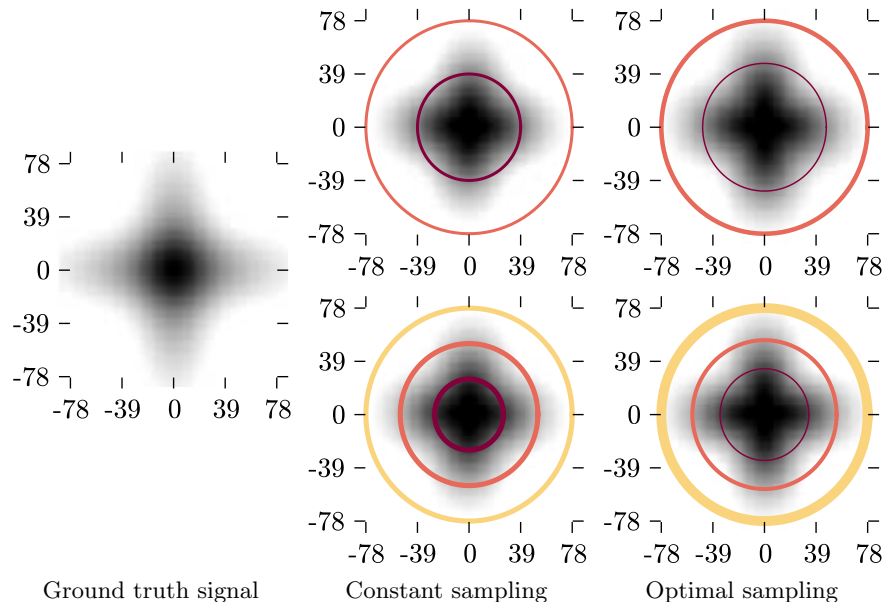
Fig. 6. 2 shell (top) and 3 shell (bottom) sampling in action, for the reconstruction of a synthetic diffusion signal corresponding to a mixture of Gaussian, simulating fiber crossing. The circles represent the sampling shells, and the line widths are proportional to the number of points per shell.

5 Conclusion

In this work, we develop a computational framework for optimal design of experiment in diffusion MRI. For the reconstruction of 1D, spherical and 3D signal, we propose sampling scheme with minimal condition number. Monte-Carlo simulations confirm this result, as the signal to noise ratio of the parameters estimated from optimal sampling scheme is improved with respect to conventional sampling scheme, for the same number of acquisitions.

As a conclusion to this study, we claim that a sampling method is optimal for a reconstruction in a given basis and a given order. In addition to the technical and physical limitations of the imaging system, the choice of the type of reconstruction must be taken into account when designing the acquisition protocol.
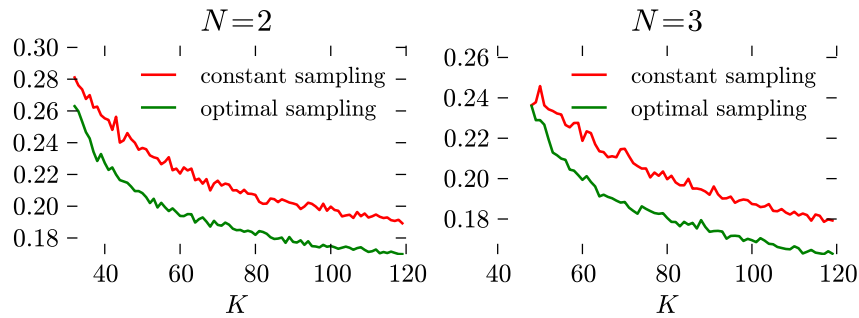
Fig. 7. Mean squared error for a synthetic diffusion signal corresponding to a mixture of Gaussian, with Rician noise (SNR=25).

References

1. Jones, D., Horsfield, M., Simmons, A.: Optimal strategies for measuring diffusion in anisotropic systems by MRI. Magn Reson Med **42**(39) (August 1999) 515 – 525
2. Jansons, K.M., Alexander, D.C.: Persistent angular structure: new insights fom diffusion magnetic resonance imaging data. Inverse Problems **19** (2003) 1031–1046
3. Koay, C.G.: A simple scheme for generating nearly uniform distribution of antipodally symmetric points on $\mathcal{S}^2$. J. Comput. Science **2**(4) (2011) 377–381
4. Papadakis, N.G., Xing, D., Huang, C.L., Hall, L.D., Carpenter, T.A.: A comparative study of acquisition schemes for DTI. J Magn Reson **137**(1) (1999) 67–82
5. Skare, S., Hedehus, M., Moseley, M.E., Li, T.Q.: Condition number as a measure of noise performance of diffusion tensor data acquisition schemes with MRI. J Magn Reson **147**(2) (December 2000) 340–352
6. Caruyer, E., Cheng, J., Lenglet, C., Sapiro, G., Jiang, T., Deriche, R.: Optimal design of multiple q-shells experiments for diffusion MRI. In: MICCAI Workshop on Computational Diffusion MRI - CDMRI'11, Toronto, Canada (September 2011)
7. Assemlal, H.E., Tschumperlé, D., Brun, L.: Evaluation of q-space sampling strategies for the diffusion magnetic resonance imaging. In: MICCAI, London (2009)
8. Portnoy, S., Ye, W., Entezari, A., Blackband, S.J., Vemuri, B.C.: A novel interlaced sampling scheme for multi-shell q-space MR microscopy. In: ISMRM. (2011)
9. Daducci, A., McEwen, J., Van De Ville, D., Thiran, J.P., Wiaux, Y.: Harmonic analysis of spherical sampling in diffusion MRI. In: ISMRM. (2011) 3929
10. Ozarslan, E., Koay, C., Basser, P.: Simple harmonic oscillator based estimation and reconstruction for 1D q-space MR. In: ISMRM. Volume 16. (2008) 35
11. Descoteaux, M., Angelino, E., Fitzgibbons, S., Deriche, R.: Regularized, fast, and robust analytical q-ball imaging. Magn Reson Med **58**(3) (2007) 497–510
12. Assemlal, H., Tschumperlé, D., Brun, L.: Efficient and robust computation of pdf features from diffusion MR signal. Medical Image Analysis **13**(5) (2009) 715–729
13. Abramowitz, M., Stegun, I.A.: Handbook of mathematical functions. Dover (1970)
14. Delsarte, P., Goethals, J., Seidel, J.: Spherical codes and designs. Geometriae Dedicata **6** (1977) 363–388 10.1007/BF03187604.
15. Goethals, J.M., Seidel, J.J.: Cubature formulae, polytopes and spherical designs. In Coxeter, H., Davis, C., Grünbaum, B., Sherk, F., eds.: The Geometric vein: the Coxeter festschrift. Springer-Verlag, New York (1981) 203–218
16. Anonymous: -. In: -. (-)